



Wired threaded inserts in joints with steel screws and aluminium nuts: A parametric study on their effectiveness

Venanzio Giannella^{a,*}, Davide Romano^b, Maurizio Greco^b, Raffaele Moliterno^b, Raffaele Sepe^a, Enrico Armentani^c

^a Department of Industrial Engineering, University of Salerno, Fisciano (SA), Italy

^b MBDA Italia S.p.A., Bacoli (NA), Italy

^c Department of Chemical, Materials and Production Engineering, University of Naples "Federico II", Naples, Italy

ARTICLE INFO

Keywords:

FEM
Joint
Nut
Wired threaded inserts
Parametric study

ABSTRACT

The aim of this research was to investigate on bolted joints characterized by steel screws and aluminum nuts by means of numerical simulation. 2D and 3D CAD/FEM parametric models were developed in order to determine the preload distribution in joints with and without a Wired Threaded Inserts (WTI), so as to compare the trend of the stress distributions and the amount of load applied to each thread. The operating mechanisms and the effectiveness of a WTI were investigated in a parametric study by means of which the most important factors of the joint (materials, class, diameter, Engagement Ratio (ER), tolerance bands) were varied.

1. Introduction

In the last century, the use of light alloys in modern industry and its applications increased significantly, in light of the possibility that derives from reducing the weight of structures [1–2]. These are used in numerous applications of technological interest, from the aerospace sector to the consumer industry, such as, for example, in the production of hardware components of electronic equipment. In some cases, light alloy components are drilled and subsequently threaded to allow the screwing of steel screws directly on them. This type of technological application often leads to thread stripping problems, due to the low strength and surface hardness of light alloys nuts (e.g. aluminium). At the same time, the general trend that is pushing towards the downsizing of components for reducing costs, weights and dimensions, coupled with the aim of achieving continuously higher load-bearing capacity, poses high criticalities in the design of joints with a steel screws on aluminium nuts. In the 1970s, Alexander's studies [3] investigated the phenomenon of thread stripping in the absence of inserts. This occurs when the material of the nut is relatively weak and at the same time the Engagement Ratio (ER, the ratio between length of the engaged screw thread and diameter of the screw) is low. A low ER can lead to an incorrect preload distribution, exposing the thread, partially or entirely, to high stresses that can lead to permanent plastic deformations or breakage of the nut thread. Nowadays, the commonly used approach to solve this type of

problem is to increase the ER value with respect to the value used in applications with steel nuts, so as to achieve a better redistribution of the preload. In this regard, Crococo [4] has conducted a study in order to assess how increasing the ER benefits stripping thread issues. On the other hand, helical inserts with rhomboid section called threaded inserts [5–6], interposed between nut and screw threads, can be an option to cope with stripping and other phenomena related to the poor mechanical properties of these alloys. These are used for different purposes, mainly including the reduction of friction at the screw-insert interface compared to the values measured at the screw-nut interface (without threaded inserts). Furthermore, they allow the reduction of torsional stresses in the tightening phase, in turn increasing the fatigue life of the joint [4]. Threaded inserts are also used to improve the preload distribution, i.e. to reduce the percentage of total preload acting on the initial threads. From the available datasheets [5], it is clear that Wired Threaded Inserts (WTIs) can reduce the preload from 50 % to 30 % on the first thread. However, despite the high technological relevance and the wide diffusion of threaded inserts, to date there are no further data or analytical reports for the sizing of the joints that foresee their use. At the same time, numerous predictive analytical models that allow to evaluate stresses and preload distributions in the threading of joints without WTIs are available. The first of these analytical models was developed by Sopwith in 1948 [7] who obtained the load distribution along the thread helix by analysing the strain distribution, in turn

* Corresponding author.

E-mail address: vgiannella@unisa.it (V. Giannella).

deducing that the distribution of load along the length of a nut was not uniform due to the strains set up in the bolt and nut. This method can be utilized for both the bolt and nut case and the turnbuckle case with symmetrical triangular thread forms.

Since [7], numerous other studies have been conducted [8–32]. In the literature currently available, the forecasting models of Yamamoto [8] and Wang and Marshek [33–34] stand out. Wang and Marshek developed a predictive model that takes into account of the nonlinear behaviour of the nut material assuming a plastic behaviour without strain hardening. They schematized the thread as a series of elements of specific stiffness, placed in series and in parallel. The accuracy of the analytical models of Yamamoto and Sopwith was studied by S. Lu [26], who compared the numerical results obtained using the Finite Element Method (FEM) with the results obtained using the models of Yamamoto and Sopwith, ascertaining their accuracy in the elastic field. Nonetheless, in all cases none of the studies conducted analyses on the effectiveness of WTIs, nor evaluated the influence of these in varying the preload distribution on the threads.

To date, the major reference guideline for sizing threaded joints is VDI 2230 [35], which presents various analytical reports for sizing joints with and without threaded inserts. Nonetheless, the attention paid to the technological aspects, to the sizing, and to the operating principles of the joints with threaded inserts, is somewhat sparse and incomplete. In the absence of predictive models for studying joints with WTIs in the non-linear field, this work aimed to investigate how the preload distribution varies and which are the factors that most influence it when WTIs are used. The operating mechanisms and the effectiveness of WTIs were investigated in a parametric FEM study where the most important factors of the joint (materials, class, diameter, Engagement Ratio (ER) of screw, tolerance bands of nut) were varied.

2. Materials and Methods

This parametric study was conducted through FEM simulations by varying the factors that typically affects the preload distribution in threaded joints. Axisymmetric 2D and 3D FEM models were developed and compared with the particular aim of calibrating and validating the 2D model, so as to eventually use it to conduct the parametric analysis. Such validation procedure was developed also with the aim of comparing the current results with those available in literature [4] as a further element of validation. 2D model validation was essential in order to reduce the computational burden for the consecutive parametric analysis, hence to reduce runtimes. The CAD model was developed using the PTC Creo Parametric software and then imported into ANSYS Workbench to conduct numerous FEM analyses. Figs. 1–2 show geometry and some figures of 2D and 3D models with/without the modelling of the WTI. Fig. 3 reports a schematic of the boundary conditions.

Due to the impossibility of carrying out experimental tests, the

calibration and validation of the models was performed by replicating the results obtained with the 2D model reported in [4]. This allowed to understand the variations between the two models both for cases with and without a WTI. The 2D model was based on the axial-symmetry of the geometry around screw axis and neglects the continuous thread helix approximating it to a discontinuous series of consecutive threads. Similarly, two further FEM models were developed with the addition of a WTI. Both 2D and 3D models comprised a partially threaded-shank screw without the head. The portion of threaded material (lower flange) consisted of a cylindrical ashlar of material. At last, a support was modelled (upper flange) which was used to simulate the contact condition between the two screwed flanges. The thread-type is metric in accordance with ISO 68 [36]. To simulate the most common real operating conditions, the tolerance bands for the thread of the nut and of the screw were considered by considering the indications contained into the ISO 965 [37]. A medium tolerance quality (the most frequent) was chosen for the threaded holes. A class 6 was chosen for the screw, whereas classes 6 and 7 were chosen for the threaded hole with $ER < 2$ and $ER = 2$ respectively. Tolerance combination H/g (the most frequent) was selected to warrant a sufficient overlap and clearance of the coupling, following the recommendations of the ISO Standards. Three different configurations were considered by changing ER from 1, 1.5 and 2. The main dimensions of screw and nut when the ER changes were listed in Table 1. The nut is made of 2017 aluminum alloy, the sleeve is made of 7075 aluminum alloy, whereas the screw is made of a steel class 12.9.

Fig. 4 shows details of the FEM mesh for the 2D and 3D models. FEM mesh of 2D model comprised 6-noded triangular elements (PLANE 183 in Ansys) with average mesh sizes set to 0.1 mm for screw/nut, 0.25 mm for the sleeve and a refinement to 0.05 mm close to the threads. FEM mesh of 3D model comprised 20-noded tetrahedral elements (SOLID 186 in Ansys) for which different mesh sizes were tested. The screw preload was defined by using an axial force of 12.28 kN acting on the upper face of the threaded-shank, according to literature data [4]. Material properties were defined as linear-elastic for the sleeve and elastic-plastic (by means of a bilinear isotropic hardening model) for all the other parts.

The small differences in the results obtained in literature [16] between 2D and 3D models suggested to use the 2D axisymmetric FEM model to conduct such a parametric analysis. This choice was also driven by the reduced computational burden and consequently by the required runtimes. Once validated the 2D model, this was used to perform a parametric analysis in such a way to study the effectiveness of the WTI in the joint. Multiple parameters were varied for such analyses in such a way to quantify their influence on the preload distribution and on the stress in the nut. Such parameters were:

- materials of nut and WTI,
- diameter of screw and nut,

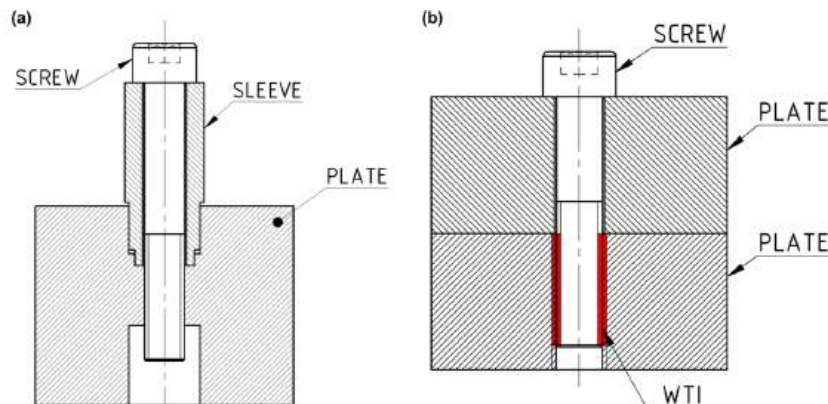


Fig. 1. Schematics of the considered joints: (a) geometry used as comparison with literature [4], (b) geometry used subsequently.

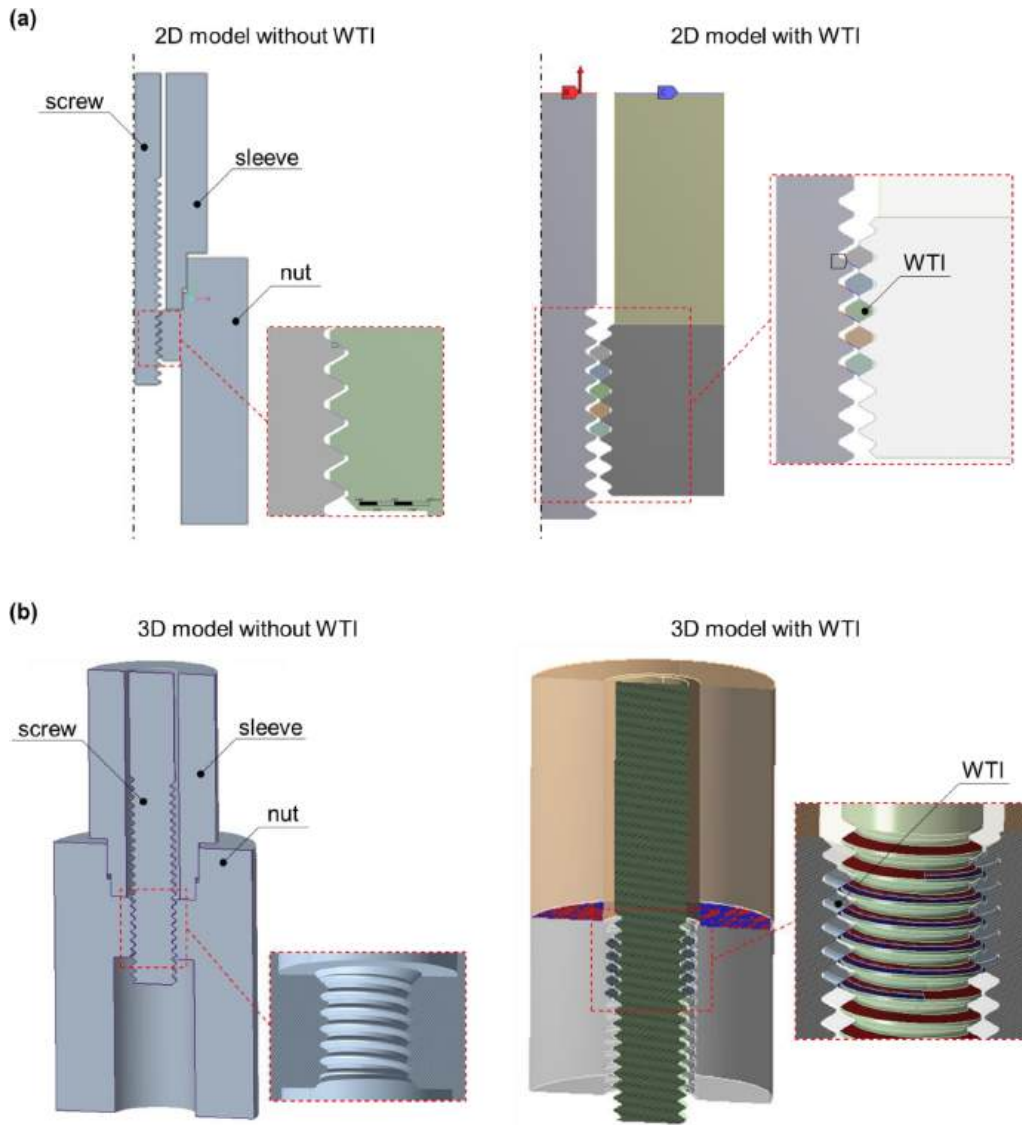


Fig. 2. (a) 2D axisymmetric FEM model with/without WTI; (b) 3D FEM model with/without WTI.

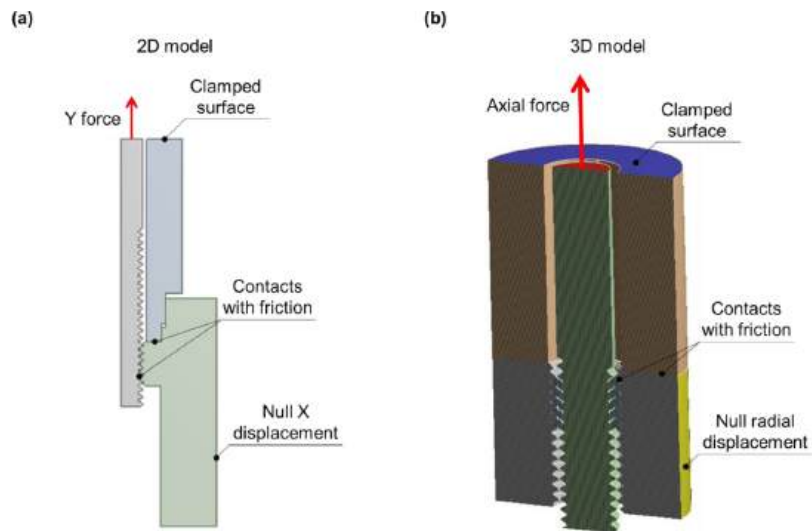


Fig. 3. FEM boundary conditions.

Table 1
Threaded components dimensions.

ER	Screw		Nut	
	Pitch diameter [mm]	Major diameter [mm]	Pitch diameter [mm]	Major diameter [mm]
1.0	5.268	5.884	5.425	5.035
1.5	5.268	5.884	5.425	5.035
2.0	5.268	5.884	5.425	5.067

- ER value,
- tolerance class of the nut,
- steel class of the screw.

The applied preload, in accordance with the suggested value reported in the ECSS guideline [38], was calculated considering a coefficient of utilisation γ of 0.65. As per the validation process, also for the parametric analyses PLANE 183 elements were chosen since it was found that the results were highly mesh-dependent, especially for the threads area. Local mesh size was parameterized according to the thread pitch (mesh sizes between 1/5th and 1/10th of the pitch, with a refinement to 1/20th in the thread area). On average, models comprised between 350k and 1000k nodes depending on joint and screw dimensions. Both during calibration and parametric analysis, the contacts

were set as frictional with friction coefficient depending on the interface couple materials, see Table 2. Such coefficients were defined according to literature [35,39]. Material properties of all materials were listed in Table 3.

M3, M6 and M10 screw sizes were considered since with these dimensions it was possible to keep ER almost constant when varying the number of engaged threads. The dimensions of major and pitch diameter for screw and minor and pitch diameter of nut were listed in Table 4. Screw sizes and threaded hole sizes were shaped according to a collocation in the middle of their tolerance bands, so as to reproduce the most frequent condition. A class 6 was chosen for the screw and classes 4 and 6 were chosen for the threaded hole independently of ER. Tolerance position combination H/g (the most frequently used) was selected.

A total of 432 different configurations were investigated in this parametric study (around 75 hours of runtime).

3. Results

3.1. Validation of 2D/3D models

Fig. 5 shows the von Mises stress distributions for 2D and 3D FEM models for ER equal to 1 and 2 with and without a WTI. It can be noticed that the stresses calculated with the 2D model were very accurate and in

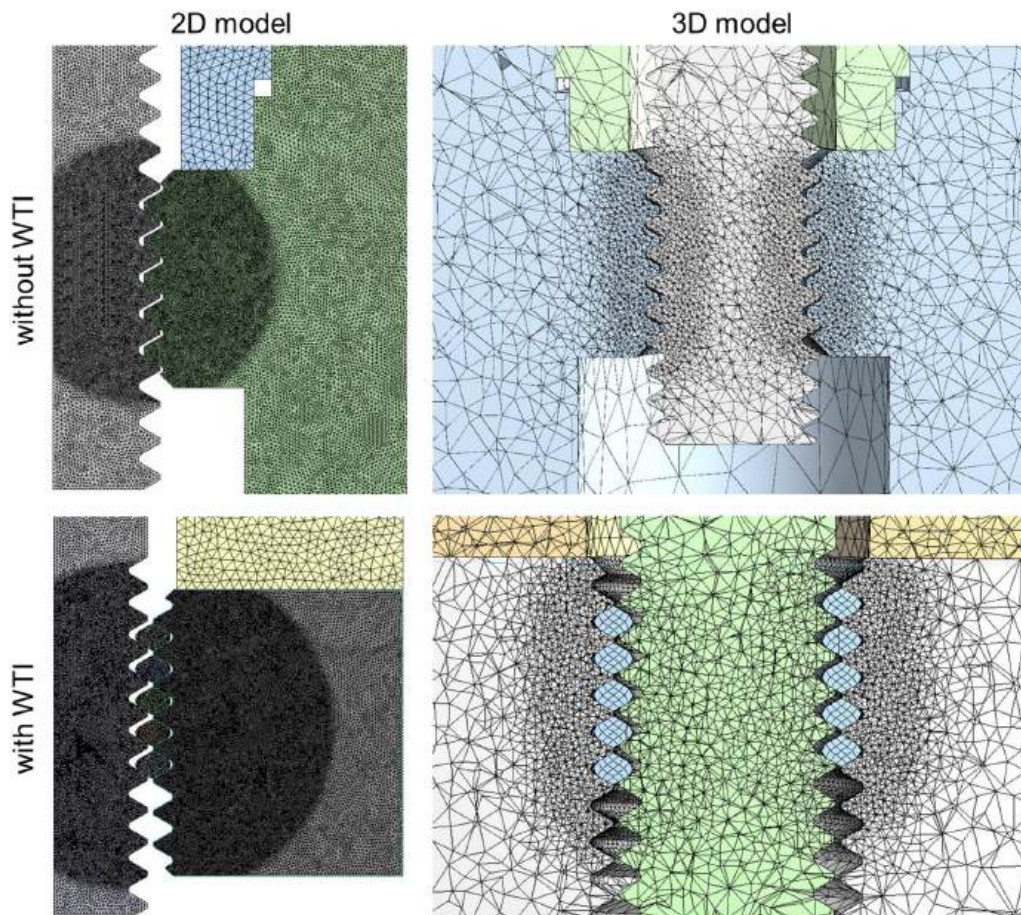


Fig. 4. FEM meshes for the 2D and 3D models with/without WTI.

Table 2
Friction coefficients.

Interface	Steel - Steel	Steel - Aluminium	Steel - Bronze	Bronze - Aluminium	Aluminium - Aluminium
Friction coefficient [-]	0.16	0.19	0.21	0.25	0.21

Table 3
Main material properties for all the considered materials.

Component	Material	Young's modulus E [GPa]	Yield stress σ_y [MPa]	Ultimate stress σ_u [MPa]	Elongation at rupture ϵ_u [-]
WTI	A2 steel	207	270	650	54
	Bronze	115	260	470	20
	Aluminium	72	165	275	10
Nut	Aluminium	72	275	427	22
	2017-T3				
	Aluminium	72	345	485	18
	2024-T3				
	Aluminium	72	275	310	17
Screw	6061-T6				
	Aluminium	72	485	540	7
	7075-T6				
	C40 steel	207	500	800	15
	8.8 class	207	640	800	12
	10.9 class	207	900	100	9
	12.9 class	207	1080	1200	8

a sound agreement with those calculated with the 3D model, for both cases with and without the WTI. For cases with $ER = 1$, stresses were on a large area significantly higher than the yield strength of the nut material (275 MPa), both for cases with and without the WTI. Moreover, it is clear that the stresses in the threads for the configuration with $ER = 1$

and without WTI, replicate the failure mode verified in the experimental tests reported in literature [4]. The results of the load distributions on the engaged threads, normalized with respect to the total preload, were shown in Fig. 6 wrt. the 3D model. Fig. 7 compares the same results among the 2D and 3D models with/without WTI for three ER values.

For cases without WTI, large plasticization occurs over the entire nut length for $ER = 1$, hence involving all the engaged threads. On the other hand, for $ER = 2$ without WTI, only the first two threads are affected by a slight localized plasticization, whereas the remaining ones tolerated the preload remaining well below the yield strength. This behaviour can be explained taking into account the force necessary to deform the thread plastically. This is about 20 % of the total preload, according to the model in [16]. This value varies slightly with the variation of the number of engaged threads (for materials that do not have a strong work hardening) whereas it is highly dependent on the thread size and the material of the nut. Once this critical value is exceeded, the succeeding tooth starts to deform plastically, the force acting on it settles on the critical value, and the preload is distributed on the subsequent tooth. This phenomenon can also be deduced from Fig. 6, where it is reported the preload distribution among the threads at the preload increasing. As a matter of fact, it can be noticed that increasing progressively the preload, there is an asymptotic value of the percentage of total preload acting on the threads, both with and WTI.

For cases with WTI, it can be seen from Fig. 7 that, for $ER = 1$, there were no appreciable variations in the preload distribution, whereas

Table 4
Threaded components dimensions (middle tolerance bands) in accordance with ISO 965.

Nominal diameter [mm]	Pitch [mm]	Screw (6 g)		Nut (6H)		Nut (4H)	
		Pitch diameter [mm]	Major diameter [mm]	Pitch diameter [mm]	Major diameter [mm]	Pitch diameter [mm]	Major diameter [mm]
3	0.5	2.618	2.902	2.726	2.530	2.706	2.504
6	1.0	5.268	5.884	5.425	5.035	5.396	4.992
10	1.5	8.928	9.850	9.116	8.526	9.082	8.472

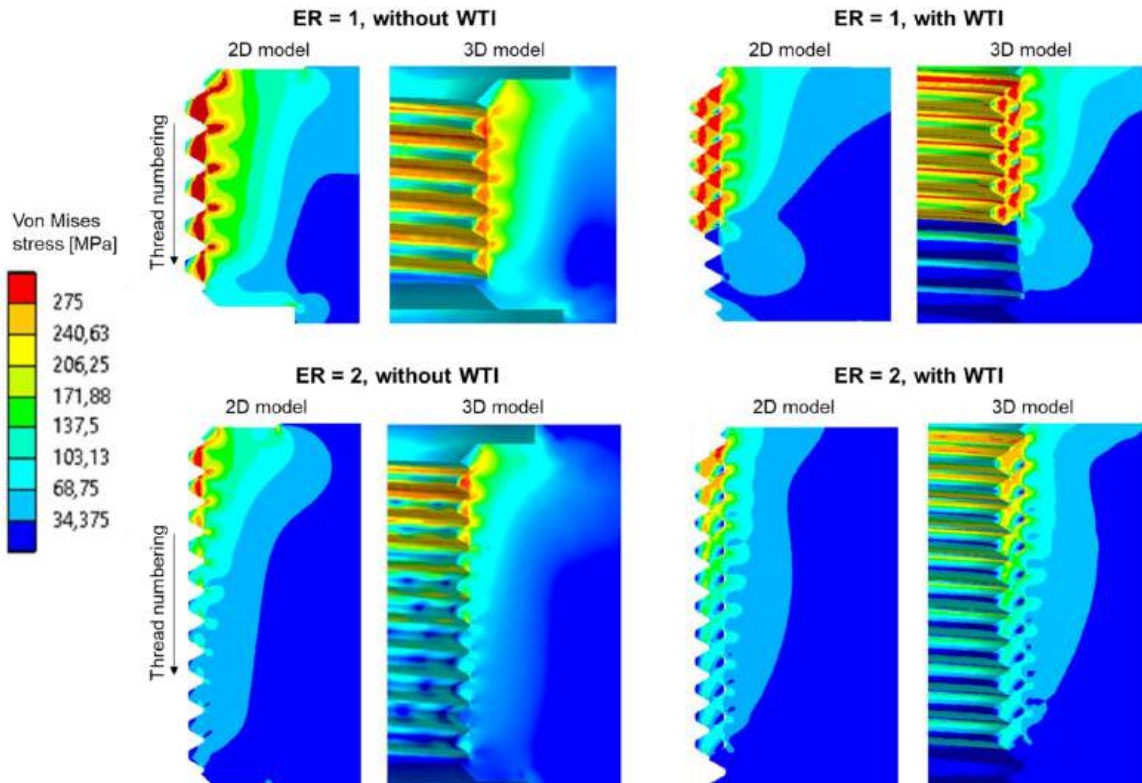


Fig. 5. Comparison of 2D/3D von Mises stress fields [MPa] for different joint configurations.

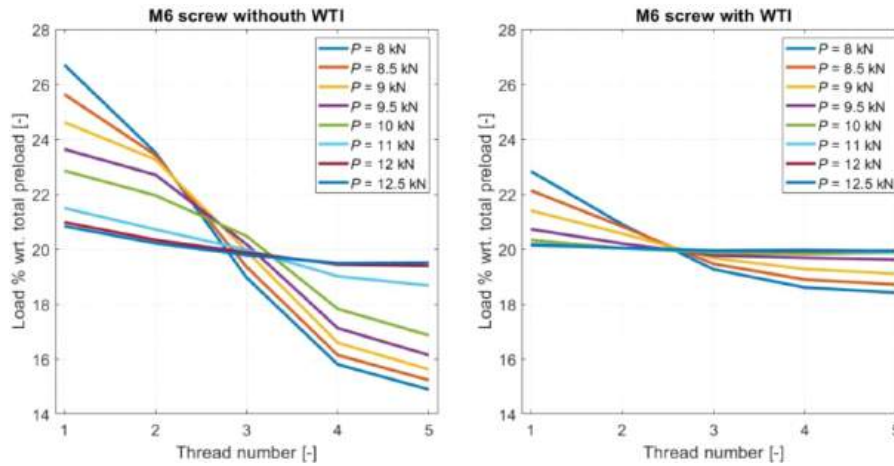


Fig. 6. Load distribution along threads as a function of total preload ($ER = 1$, 3D model).

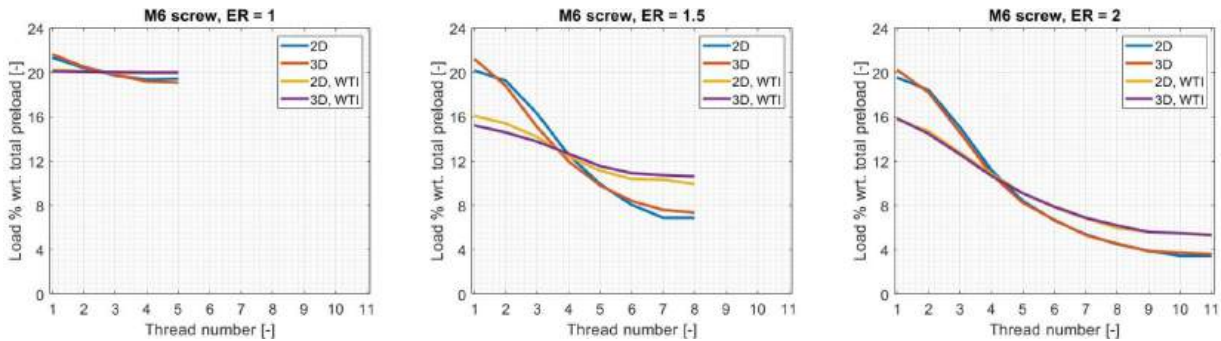


Fig. 7. Preload distribution as a function of ER; comparison among 2D and 3D models.

higher variations were noticed for cases without WTI. On the other hand, for cases with $ER = 1.5$ and 2, almost similar improvements were observed on the first threads between cases with/without WTI. The same holds true also with reference to the von Mises stresses shown in Fig. 5, where larger variations were noticed for the case with $ER = 2$, rather than for the case $ER = 1$. It is also worth noting that there is a “minimum” ER over which benefits start to be appreciated (usually around ER

$= 1.5$). After exceeding such a minimum ER, further increments do not contribute to a further unloading of the first threads.

The Pareto chart of the results obtained during this parametric investigation was shown in Fig. 8. Y-axis reports the parameters grouped and listed in a descending order in terms of importance (groups at top of the chart are those having the highest impact on the calculations). From a first statistical analysis, it was clear that the parameters that most

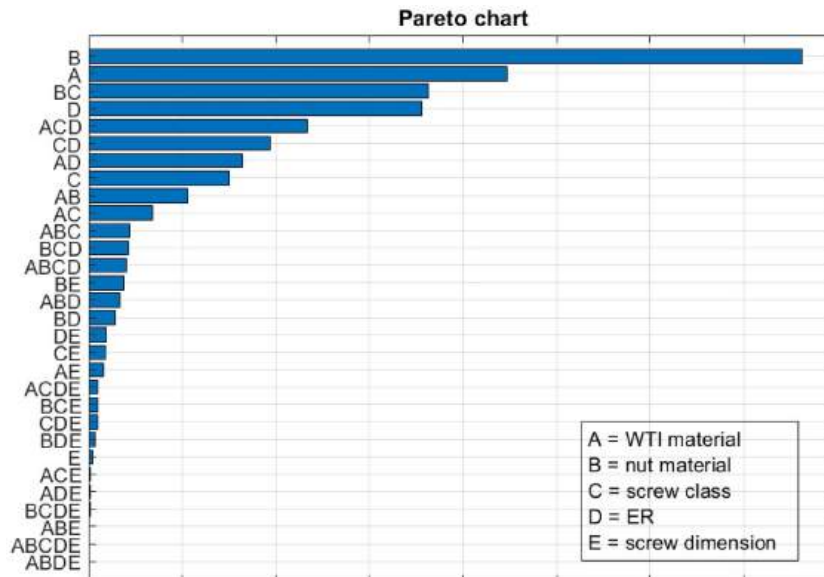


Fig. 8. Pareto chart for all cases with WTI.

influence the results were, in order of importance:

1. the material selected for nut and WTI,
2. the engagement ratio ER,
3. the steel screw class.

The size of the screw did not significantly affect the results.

Results of the parametric analyses were reported in the following sections. All results were centred on the parameter L_i / P , where L_i represents the load on the i -th tooth whereas P represents the total preload acting on the joint, hence $\sum_i L_i / P = 100\%$. Reducing such L_i / P value for the first teeth mean to a better redistribution of the load on all the other threads. Larger reductions on first threads are therefore beneficial for the life of the joint.

3.2. Comparison among different materials

The difference between the load amount per tooth L_i with respect to the total preload P is shown in the following Figs. 9-10 for different materials of nut and WTI. As stated before, negative value indicates a decrease in the load acting on the thread, i.e. an improvement. From results of Fig. 9, it is clear that the aluminum WTI contribute to the greatest reductions of the loads acting on the first threads, compared to A2 steel and bronze. This is more significant especially in cases with $ER > 1$. Indeed, the effectiveness of a WTI does not depend on its material in case with $ER = 1$. Besides, the variation of the preload distribution does not change when the WTI material changes regardless of the materials used for the nut. It is also clear from Fig. 9 that the load reduction on the first threads is higher for nut materials with a high yield stress (such as C40 steel and 7075 aluminum alloy). However, the aluminum WTI

works better than those in bronze or steel for all the considered cases.

3.3. Comparison among different screw diameters

Fig. 10 shows the variations of the preload distribution as a function of screw diameter and WTI material. For all cases, it is observed that there is no correlation between the screw diameter and the variation in the preload distribution when a WTI is used. This can also be inferred from the Pareto charts reported in Fig. 8.

3.4. Comparison among different screw diameters

Fig. 11 shows the variation of the preload distribution for three ER values as a function of material for nut and WTI. As expectable, it can be said that, as the ER increases, higher benefits can be achieved. There are improvements in the variation of the preload distribution (i.e. an increase in the effectiveness of the WTI) for all cases with $ER > 1.5$. For example, in all cases analyzed with $ER = 2$ and aluminum WTI, the maximum effectiveness is greater with that achieved with bronze or steel WTIs. Cases with $ER = 1$ are those that show a minor variation in the preload distribution, regardless of the configuration taken into consideration. These outcomes are in agreement with those already reported in Figs. 9, 10. Under the same ER, the variation of the preload distribution is greater in cases with C40 steel nut compared to cases with 6061 aluminum alloy nuts.

3.5. Comparison among different screw classes

Fig. 12 shows the trends of the variation of the preload distribution as the class of the screw changes for different configurations of screw

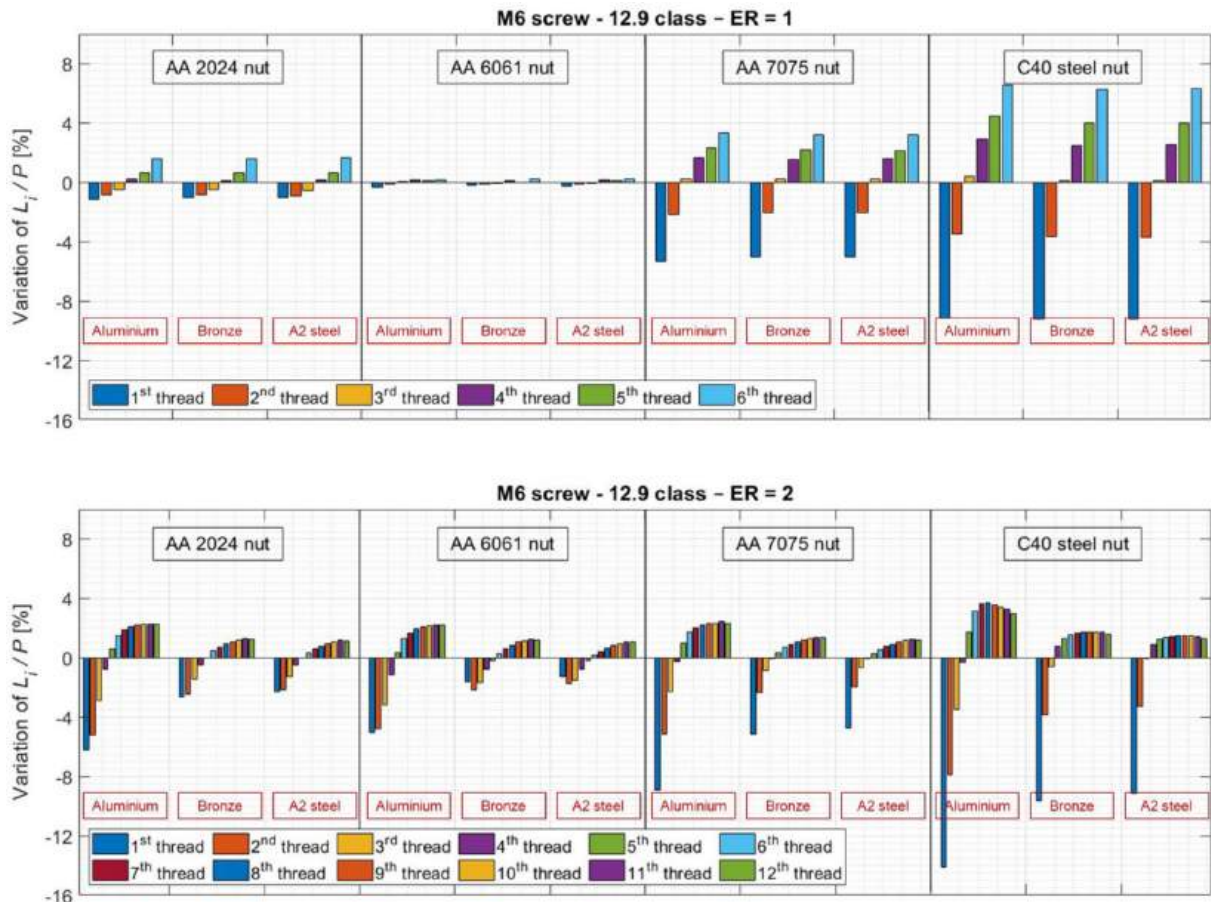


Fig. 9. Variation of the preload distribution as a function of nut material (black boxes) and WTI material (red boxes).

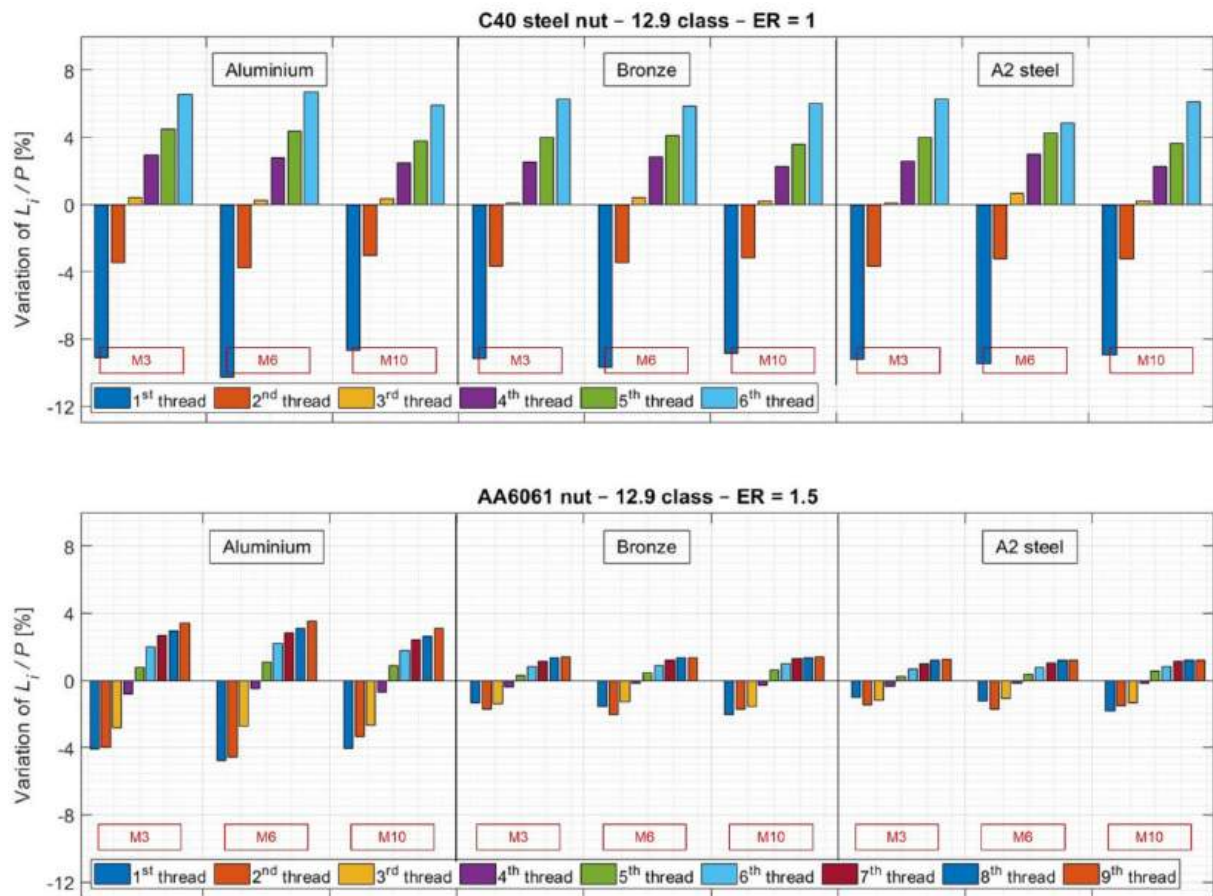


Fig. 10. Variation of the preload distribution as a function of WTI material (black boxes) and screw diameter (red boxes).

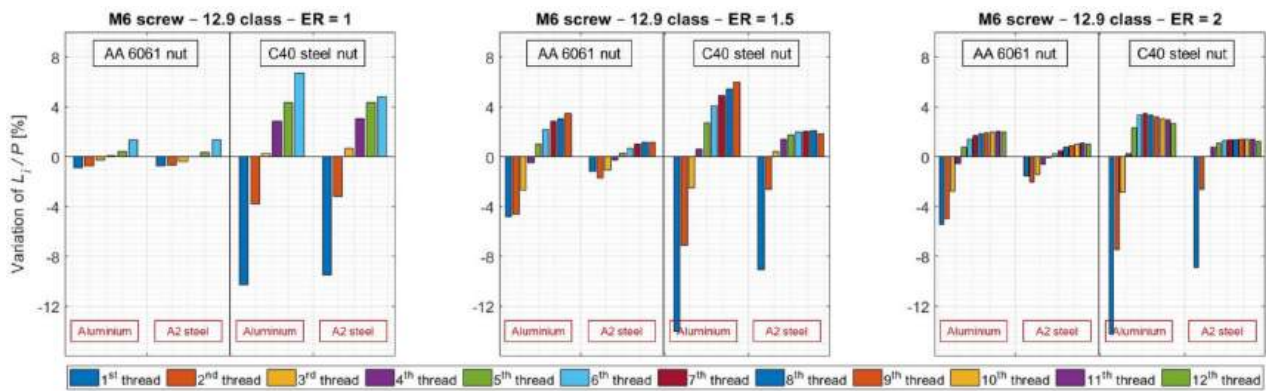


Fig. 11. Variation of the preload distribution for three ER values as a function of nut material (black boxes) and WTI material (red boxes).

diameter and material of the nut. It can be noticed that the results are almost similar to those reported with reference to the variation of the screw diameter, see Fig. 10. In both cases (12.9 and 8.8 classes), there is a higher effectiveness of a WTI on a nut material such as C40 steel. For the 6061 aluminum alloy with class 8.8, it is observed that the WTI allows for an increase in the variation of the preload distribution for the case with $ER = 1$, whereas no appreciable variations are reported for $ER = 2$. At the same time, for the case with C40 steel and 8.8 class, a reduction in the effectiveness of the WTI is observed for cases with $ER = 2$ whereas, once again, negligible variations can be noticed for $ER = 1$.

3.6. Variation of the nut tolerance bands

The influence of the nut threads tolerance band was analyzed for cases without WTI, in such a way to evaluate the influences of this parameter on the preload distribution. It can be observed from Fig. 13 that this does not considerably influence the preload distribution, both in the elastic and in the elastic-plastic fields. Results of Fig. 13 were calculated considering AA6061 as material of the nut. Even lower variations were calculated by considering C40 steel and were not reported here for brevity.

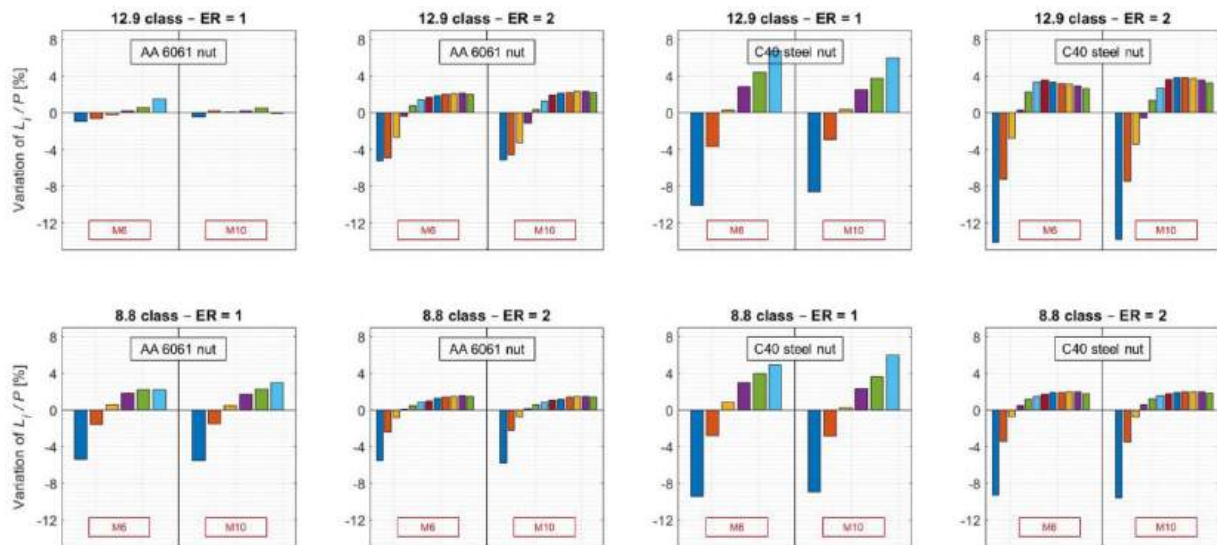


Fig. 12. Variation of the preload distribution for two screw classes as a function of nut material (black boxes) and screw diameter (red boxes).

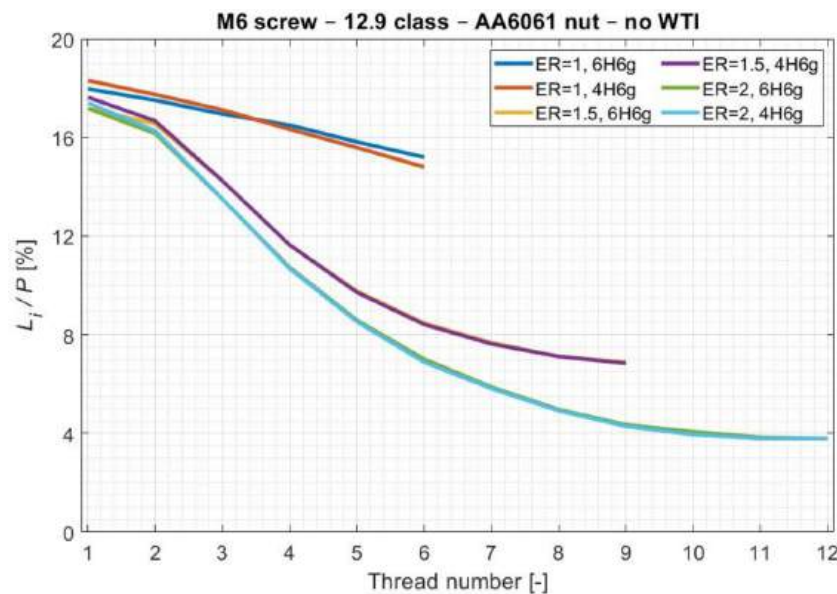


Fig. 13. Tolerance bands variation for cases without WTI.

4. Conclusions

A parametric study on the effectiveness of wired threaded inserts in joints characterized by a steel screw and an aluminium nut was presented in this document. To this aim, 2D and 3D numerical simulations were developed and the results cross-compared with those available in literature. The error committed using 2D axis-symmetric models instead of fully 3D models is negligible for all configurations with/without considering a WTI. The operating mechanisms and the effectiveness of a WTI were investigated in a parametric study by means of which the most important factors of the joint (materials, class, diameter, Engagement Ratio, tolerance bands) were varied.

The effectiveness of using a WTI for reducing the preload distribution is not a constant, as declared by many manufacturers. For all cases, the WTI has proved to be beneficial in the reduction of the stresses especially at the root of nut threads. A ER value around 1.5 was calculated as the “minimum” value above which benefits in using a WTI are noticed, this especially with nuts consisting of alloys with low yield stress used in

combination with class 12.9 steel screws. The WTI effectiveness does not vary with the screw diameter. In general, with other factors being equal, the effectiveness of an aluminum WTI is greater than that achieved with bronze or A2 steel. For all cases, the variation of the nut tolerance class from 6H to 4H did not lead significant variations in the preload distribution.

CRedit authorship contribution statement

Venanzio Giannella: Writing – review & editing, Writing – original draft, Visualization. **Davide Romano:** Writing – original draft, Formal analysis, Data curation. **Maurizio Greco:** Visualization, Supervision, Methodology, Conceptualization. **Raffaele Moliterno:** Validation, Supervision, Project administration, Conceptualization. **Raffaele Sepe:** Writing – review & editing, Writing – original draft, Visualization, Supervision. **Enrico Armentani:** Visualization, Supervision, Methodology, Conceptualization.

Declaration of competing interest

The authors declare that they have no known competing financial interests or personal relationships that could have appeared to influence the work reported in this paper.

Data availability

The authors do not have permission to share data.

References

- [1] R. Sepe, V. Giannella, N. Razavi, F. Berto, Characterization of static, fatigue and fracture behaviour of the aluminium-lithium alloy Al-Li 2198-T851, *Int. J. Fatigue* 166 (2023) 107265, <https://doi.org/10.1016/j.ijfatigue.2022.107265>.
- [2] R. Sepe, V. Giannella, P. Mazza, E. Armentani, N. Razavi, F. Berto, Fatigue fracture tests on Al-Li 2198-T851 specimens under mixed-mode conditions, *Procedia Struct. Integrity* 39 (C) (2021) 546–551, <https://doi.org/10.1016/j.prostr.2022.03.127>.
- [3] E.M. Alexander, Analysis and design of threaded assemblies, *SAE Trans.* 86 (Section 3) (1977) 770404–770718, pp. 1838 - 1852.
- [4] D. Crococolo, M.D. Agostinis, S. Fini, G. Olmi, Steel screws on aluminium nuts: different engagement ratio tapped threads compared to threaded inserts with a proper tolerance choice, *Tribol. Int.* 138 (2019) 297–306.
- [5] BOLLHOFF, Thread technology for high-strength fastenings - metric threads. Available online: <https://www.ret.hu/media/product/34110/636028/helico-il-plus-en-0100.pdf>.
- [6] C. Company, Handbok om skruvforband, 2020. [Online]. Available: http://www.collycomponents.se/wp-content/uploads/2017/06/HANDBOK_skruforband.pdf.
- [7] D Sopwith DG, The distribution of load in screw threads, *Proc. Inst. Mech. Eng.* 159 (1) (1948) 373–383, https://doi.org/10.1243/PIME_PROC.1948.159.030.02.
- [8] Y. A., The Theory and Computation of Thread Connection, Tokyo, 1980, pp. 39–54.
- [9] M. Allison, Analysis of buttress threads in a tension coupling, in: *Congress on Material Testing, Seventh Lecture, Budapest, Hung.* 2, 1978, pp. 413–416.
- [10] J.L. Bretl, R.D. Cook, Modeling the load transfer in threaded connections by the finite element method, *Int. J. Numerical Methods Eng.* 14 (9) (1979) 1359–1377.
- [11] S.C. Chapra, R.P. Canale, *Numerical Methods for Engineers*, Second Edition, McGraw Hill Book Company., 1988.
- [12] S.D. Crum, Distribution of Load Over the Threads of a Threaded Closure: Including Temperature Effects and Local Imperfections, in: *ASME, Pressure Vessels and Piping Division (Publication)*, 148, Published by ASME, New York, NY, 1988, pp. 43–53.
- [13] D. Zhang, S. Gao, S. Niu, H. Liu, A prediction method for load distribution in threaded connections, *J. Theor. Appl. Mech.* 56 (2018) 157–168. Warsaw.
- [14] T. Fukuoka, N. Yamasaki, H. Kitagawa, M. Hamada, Stress in bolt and nut, *Bull. JSME* 29 (1986) 3275–3279.
- [15] J.N. Goodier, Distribution of Load in Threads of Screws, *Trans. ASME* 62 (1940) A10–A16.
- [16] G. Yang, J. Hong, L. Zhu, B. Li, M. Xiong, F. Wang, Three-dimensional finite element analysis of the mechanical properties of helical thread connection, *Chine. J. Mech. Eng.* 26 (2013) 564–572.
- [17] M. Hetenyi, A Photoelastic study of bolt and nut fastenings, *Trans. ASME* 65 (1943) A93–A100.
- [18] R.B. Heywood, *Designing Against Fatigue of Metals*, Reinhold Publishing Co., 1962.
- [19] R.B. Heywood, *Designing By Photoelasticity*, Chapman & Hall Ltd., 1952.
- [20] B. Kenny, E.A. Patterson, Load and stress distribution in screw threads, *Exp. Mech.* 25 (3) (1985) 208–213.
- [21] W. Wang, K.M. Marshek, Determination of the load distribution in a threaded connector having dissimilar materials and varying thread stiffness, in *Mechan. Mach. Theory*, Vol 117/1, 1995.
- [22] D.L. Miller, Determination of load distribution in a threaded connection, *Mechan. Mach. Theory* 18 (6) (1983) 421–430.
- [23] A. Newport, G. Glinka, Reducing the local stresses in threaded tether connections, in: *Proceedings of the International Offshore Mechanics and Arctic Engineering Symposium 7th, 1*, Published by ASME, New York, 1988, pp. 141–147.
- [24] P. O'Hara, Finite Element Analysis of Threaded Connections, in: *Proceedings of the Army Symposium on Solid Mechanics*, Publ. by Army Materials and Mechanics Research Center, AMMRC MS 74-8, 1974, pp. 99–119.
- [25] J.-J. Chen, Y.-S. Shih, A study of the helical effect on the thread connection by three dimensional finite element analysis, *Nuclear Eng. Des.* 191 (2) (1999) 109–116.
- [26] S. Lu, D. Hua, F. Cui, P. Li, Load and stress distribution of thread pair and analysis of influence factors, in: *Journal of Physics: Conference Series* 1187, 2019.
- [27] E.E. Stoeckly, H.J. Macke, Effect of Taper on screw-thread load distribution, *Trans. ASME* 74 (1) (1952) 103–112.
- [28] M. Tanaka, K Hongo, E. Asaba, Finite element analysis of the threaded connections subjected to external loads, *Bull. JSME* 25 (200) (1982) 291–298.
- [29] M. Tanaka, K. Yamada, The behavior of fasteners under external loading, *Bull. JSME* 29 (248) (1986) 617–624.
- [30] A. Greco, A. De Luca, G. Lamanna, R. Sepe, Numerical investigation on the influence of tightening in bolted joints, *Procedia Struct. Integrity* 24 (2019) 746–757, <https://doi.org/10.1016/j.prostr.2020.02.066>.
- [31] S. Yazawa, K. Huongo. Distribution of load in the screw thread of a Bolt-Nut connection subjected to tangential forces and bending moments, in *JSME International Journal, Series I*, Vol. 31, No. 2, 1988, pp. 174–180.
- [32] V. Giannella, R. Sepe, R. Citarella, E. Armentani, FEM modelling approaches of bolt connections for the dynamic analyses of an automotive engine, *Appl. Sci.* 11 (2021) 4343, <https://doi.org/10.3390/app11104343>.
- [33] W. Wang, *Determination of Load Distributions in Threaded Connectors*, The University of Texas at Austin, 1991. Ph.D. Dissertation.
- [34] W. Wang, K.M. Marshek, Determination of load distribution in a threaded connector with yielding threads, *Mechan. Mach. Theory* 31 (2) (1996) 229–244.
- [35] VDI 2230-Part 1, 2003.
- [36] International Organization for Standardization ISO 68:1998 general purpose screw threads — Basic Profile — Part 1: Metric screw Threads, 1998.
- [37] International Organization for Standardization ISO 965:2013. ISO General Purpose Metric Screw Threads – Tolerances, Geneva, Switzerland, 2013.
- [38] Chapter 6: The Preload; Paragraph 6.2: Coefficient of Utilisation, in *ECSS-E-HB-32-23A: Threaded fasteners Handbook*, 2010.
- [39] R.T. Barrett, *Fastener Design Manual*, Nasa, Document ID 19900009424 (1990) 16. Available online: <https://ntrs.nasa.gov/citations/19900009424>.